

that the expected change in the spatial distribution function is not observed experimentally.**

The experimental results obtained can be explained under the assumption of the presence of a single, energetically distinct nuclear-active particle in the core of the extensive air shower having a primary energy less than 10^{15} ev. This particle produces then the high-energy electron-photon component in the depth of the atmosphere.⁶

This conclusion can be illustrated by the comparison of our results on the spatial distribution with the angular distribution of particles in the nucleon-nucleon interaction processes observed in photographic emulsions. Under the assumption that the extensive air showers, recorded by us, which are produced by primary nucleons of 1.2×10^{13} ev, are formed at ~ 15 km, it follows from the experimentally observed spatial distribution that the greater part of the energy released in the primary interaction is carried away by particles within a solid angle equal to $\sim 10^{-4}$ sterad. In Ref. 7, only one particle was found within the angle of 10^{-4} sterad in a nucleon-nucleon interaction at $\sim 10^{13}$ ev primary energy, the single particle evidently carrying away the greater part of

**The tendency of the spectral distribution function for showers of 10^{15} ev to be steeper, which may possibly be connected with the change of the nature of the primary nuclear interaction process for particles of 10^{15} ev⁵ needs an additional investigation.

the energy of the primary particle.

The authors wish to express their deep gratitude to Prof. N. A. Dobrotin and G. T. Zatsepin for their interest in the present work. O. I. Dovzhenko, Iu. I. Vavilov, V. V. Batov, Iu. F. Evstigneev, M. S. Tuliakina, N. S. Il'ina and other collaborators took part in the measurements. The authors wish to express to all of them their sincere appreciation.

1 Vavilov, Nikol'skii and Tukish, Dokl. Akad. Nauk SSSR 93, 233 (1953).

2 Zatsepin, Rozental', Sarycheva, Khristiansen and Eidus, Izv. Akad. Nauk SSSR Ser. Fiz. 17, 39 (1953).

3 S. Z. Belenkii, *Cascade Processes in Cosmic Rays*, GITTL, Moscow, 1948.

4 I. L. Rozental' and D. S. Chernavskii, Uspekhi Fiz. Nauk 52, 185 (1954).

5 Nikol'skii, Batov and Vavilov, Dokl. Akad. Nauk SSSR 111, 1 (1956).

6 Dobrotin, Zatsepin, Nikolskii, Sarycheva and Khristiansen, Izv. Akad. Nauk SSSR, Ser. Fiz. 19, 666 (1955).

7 Schein, Glasser and Haskin, Nuovo Cimento 2, 647 (1955).

Translated by H. Kasha
205

Nuclear Disintegrations Produced by 660 mev Protons in Photographic Emulsions

E. L. GRIGOR'EV AND L. F. SOLOV'EVA

Institute for Nuclear Problems, Academy of Sciences, USSR

(Submitted to JETP editor July 18, 1956)

J. Exptl. Theoret. Phys. (U.S.S.R.) 31, 932-938 (December, 1956)

We present experimental material from an investigation of nuclear disintegrations produced in photographic emulsion by 660 mev protons. The general features of the disintegration, the magnitude of the cross section for inelastic processes, and the distributions in energy and angle of secondary protons and alpha particles are presented. The yield of charged π -mesons per disintegration is obtained, and an approximate value is suggested for the lower limit of the cross section for emission of two charged π -mesons in a disintegration.

AT the present time there has been accumulated a large amount of experimental material from investigation of nuclear disintegrations occurring through the action of particles with energies of some hundreds of mev.

Experiments on stars in photographic emulsion, radiochemical investigations of reaction products, and experiments on scattering and absorption of

particles have enabled us to establish the quantitative features of some aspects of the process of interaction of high energy particles with nuclei, and to compare the experimental data with various pictures of the nuclear model and the mechanism of interaction. However, a detailed analysis of the experimental data is made difficult by the great variety of the processes which occur, and also by the lack

of a complete theory of the nucleus and of nuclear interactions. Despite this situation, any new factual material makes a definite contribution to the program of studying the properties of nuclear matter, especially if the experimental conditions under which it was obtained extend the scope of previous investigations. This situation has prompted

us to carry out some measurements on disintegrations produced in photographic emulsion by 660 mev protons. The fundamental questions which were investigated were the general features of the disintegration, the interaction cross section, and the distribution in angle and energy of charged particles in disintegrations.

TABLE I

Number of prongs	2	3	4	5	6	7	8	9	10	11	12	Total number of stars	Average number of prongs
All stars, %	8	17	22	18	13	9	7	3	2	1	—	1333	4.9
Stars with black tracks, %	21	24	21	15	9	4	3	1.5	1.0	0.5	—	463	4.0

DISTRIBUTION OF STARS ACCORDING TO NUMBER OF PRONGS

The distribution of stars according to number of prongs, as measured in electron-sensitive plates, is given in Table I. The distribution confirms the familiar fact that the average number of prongs per star changes very little with the energy of the incident particle; with increasing energy, the number of many-pronged stars increases somewhat.

The tracks of fast particles, mainly protons, with energy greater than 50 mev are usually called grey tracks; these tracks are produced by protons knocked out of nuclei by the primary particle. The average number of such tracks per disintegration is 0.98 ± 0.20 . The frequency of occurrence of such tracks is shown in Table II.

The grey tracks are highly collimated along the direction of the incident protons (Figure 1), with a half-width in angle of about 20° . Earlier we found¹ that the average number of prongs in distributions from 460 mev protons was 4.2. The closeness of the numbers of prongs in disintegrations produced by protons with such different energies is a reflection of the fact that the nuclear excitation changes very little with increasing energy of the primary particle. This is also evidence of the fact that the major part of the energy imparted to the nucleus by the particle is carried off in the primary interaction.

CROSS SECTION FOR INELASTIC INTERACTIONS

A count of cases of interactions of protons with nuclei was made by scanning along the tracks of

the initial protons. This method eliminates the possibility of missing such events as no-pronged stars, small-angle scattering, and one-prong stars. The results of the measurement, including the necessary corrections for elastic scattering, are presented in Table III.

In computing the total free path for light nuclei, Λ_l , and heavy nuclei, Λ_h , it was considered that 83% of the collisions occur on nuclei of silver and bromine.² The experimental ratios of the interaction cross section to the geometrical cross section of the nucleus were 0.46 ± 0.18 and 0.87 ± 0.12 for the light and the heavy nuclei respectively. Such ratios, as calculated from the semi-transparent nucleus theory, give 0.70 for light nuclei and 0.86

TABLE II

Number of grey prongs	0	1	2	3	Total no. of stars	
% of stars	. . .	29	46	21	4	1333

for heavy nuclei. Thus for the heavy component of the emulsion we find within the limits of error of the measurement agreement with the computed cross section, while for the light nuclei the respective values differ by about a factor of two: $\sigma_{\text{theor.}} \approx 2\sigma_{\text{exp.}}$

This result indicates that light nuclei are much more transparent than the theory predicts.

SLOW CHARGED PARTICLES

Slow charged particles (protons with energy less

than 50 mev, and α -particles), were studied by constructing angular and energy distributions. For this purpose, tracks of singly and doubly charged particles were measured in plates of relatively low sensitivity, which had good charge discrimination. All the singly charged particles were identified as protons, all the doubly charged particles as alpha particles. In order to consider interactions only with heavy nuclei (Ag or Br), to which the evaporation theory is reasonably applicable, we selected disintegrations containing 6 or more tracks, and with excitations above a certain limiting value. The selection was made so that the average number of black prongs per star was 7.4.

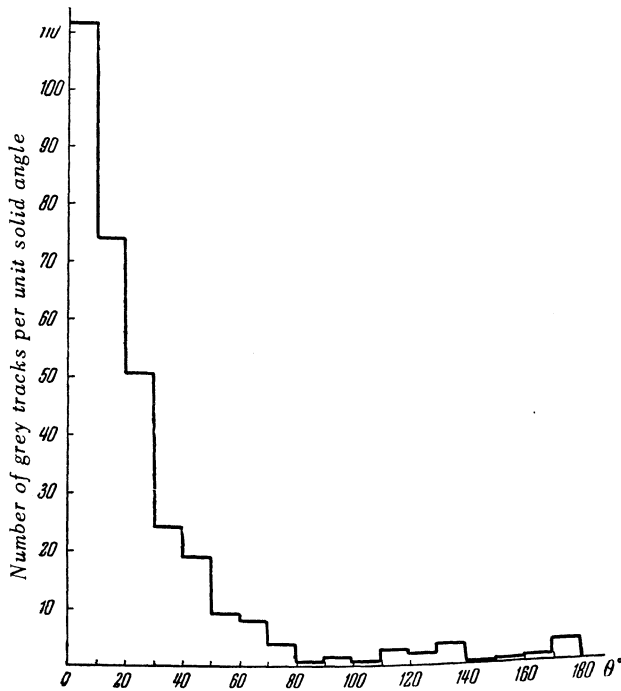


FIG. 1. Angular distribution of grey tracks. Total number of tracks = 946.

Table IV gives the ratio α/P of the number of doubly charged particles to the number of singly charged particles for stars with 6 to 8 prongs. The values for stars with a greater number of prongs are not given because of insufficient experimental material.

The results given in the Table are in agreement with the data of other work^{3,4} on stars with the same prong number, and also, as in Ref. 4, indicate a negligible change in the ratio with increase of number of particles emitted. Later it will be shown that the average number of black tracks, which was 7.4, corresponds to an excitation energy of $U = 230$ mev. The calculated⁵ value of α/P for this energy should be 0.45. If we now take account of the cascade particles (about 30% of the protons and 20% of the α -particles, cf. below), then our average ratio α/P becomes 0.42, which is not too different from the computed value.

The charged particles are not emitted isotropically, as is demonstrated by the distributions in Figures 2 and 3. If we assume that in the evaporation process the protons and α -particles are distributed isotropically, we can roughly estimate from the graphs the number of particles emitted in the cascade process. Both for the α -particles and the protons, the distributions become isotropic beyond about 100° . It then follows from the graphs that about 30% of the protons and approximately 20% of the α -particles are emitted in the cascade process. These estimates apparently give somewhat low values, since the many-pronged stars correspond to large nucleon cascades, in which the preference for the initial direction of the particle is lost as the result of the large number of collisions in the nucleus, and the recoil particles can emerge from the nucleus in various directions.

The proton energies were determined by measuring track lengths or, if the track did not end in the emulsion, by measuring the grain density. In order to make this latter method possible, we constructed a calibration curve of grain density vs.

TABLE III

Total length of tracks, in meters	26, 10	Λ , cm	39 ± 5
Number of stars	58	Λ_l , cm	237 ± 74
Number of scatterings by nuclei	50	Λ_h , cm	47 ± 7
Number of $p-p$ scatterings	3	σ_l , 10^{-24} cm ²	$0,16 \pm 0,06$
Number of disappearances of tracks	2	σ_h , 10^{-24} cm ²	$1,06 \pm 0,15$
Corrected number of all inelastic collisions			
	67	—	—

energy by measuring numbers of grains along tracks of particles stopping in the emulsion. This method

made possible the determination of energy to an accuracy of only about 20%.

For the purpose of obtaining at least partial separation of evaporation protons from recoil protons, two particle distributions were constructed, one for those emitted into the forward hemisphere and another for the backward hemisphere. The corresponding distributions are shown in Figure 4. The spectra differ from one another only in the somewhat longer tail on the high energy side for the protons emitted into the forward hemisphere. If we omit the long-range protons with energies greater than 30 mev, the spectra are characterized by the quantities given in Table V.

TABLE IV

Number of prongs	α/P
6	0.35 ± 0.04
7	0.37 ± 0.05
8	0.36 ± 0.05
Average	0.36 ± 0.05

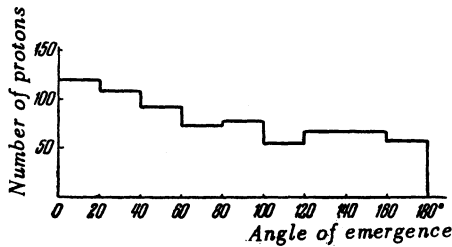
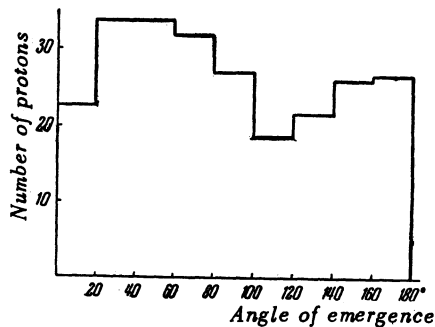


FIG. 2. Angular distribution of slow protons.

FIG. 3. Angular distribution of α -particles.

The probable energy is the same for both spectra, and agrees with the value predicted by the evaporation theory.⁵ The energy distribution of the protons emitted into the backward hemisphere is satisfactorily described by the expression

$$P(T) dT = (\bar{T} - V') \tau^{-2} \exp \{ -(\bar{T} - V') \} \quad (1)$$

with $\bar{T} = 9$ mev, $V' = 2$ mev and $\tau = 4$ mev.

The energies of the α -particles were determined from their range. In constructing the spectrum (Figure 5), corrections were made for particles not stopping in the emulsion. The principle characteristics of the spectra are given in Table VI.

The difference between the average energies for the "forward" and "backward" spectra may be caused by the participation of the α -particles in the nuclear cascade. However, this fact in combination with the observed considerable number of low-energy α -particles (far greater than the number of slow protons), may also support the assumption of preferential emission of α -particles during the initial stage of the evaporation when the nucleus is still highly excited and is moving in the direction of impact of the primary particle. In some papers⁴ it is indicated that, with increasing excitation energy, the number of slow particles increases simultaneously with the increase in number of long-range α -particles. At the same time, the value of the probable energy decreases. At the present time, the only explanation for the presence in the spectrum of slow α -particles is the assumption that the nuclear barrier is decreased. If we accept this point of view, the experimental facts presented do not contradict the assumption that the emission of α -particles occurs before the emission of protons.

TABLE V

	Average energy, mev	Probable energy, mev
Particles emitted forward .	10.2	7
Particles emitted backward .	9	7

EXCITATION ENERGY

The experimental determination of the excitation energy of the nuclei undergoing disintegration in the photoemulsion is greatly hampered by the impossibility of observing neutrons. In addition it is difficult to take account of those cascade particles which have energies in the region of energy of the evaporated particles. An estimate of the number of neutrons emitted can be made on the assumption that the final nucleus has maximum stability. This assumption can be supported experimentally from observations of decay electrons at the center of stars. Among 303 stars with prong

number $n \geq 6$, we found only 21 stars in which an electron was emitted; these represent only 7% of the total number of disintegrations. Thus the ob-

servations show that most of the nuclear mass is left in the final stable state.

Since we are here observing disintegrations of

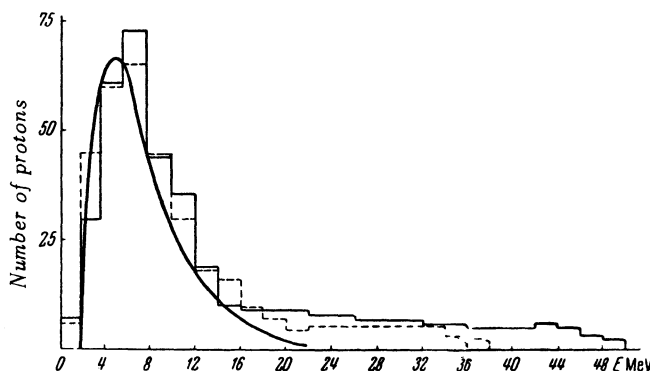


FIG. 4. Energy distribution of slow protons emitted forward (——) and backward (-----). The solid curve is computed from formula (1) with $V' = 2$ mev and $T = 4$ mev.

only Ag and Br, the initial values of A and Z , averaged over the two types of nuclei, are 94 and 41, respectively. Using the numbers found for emerging α -particles and protons, we find that on the average about 10 neutrons are emitted in each star. Knowing the average energies in the spectra of protons and α -particles, and also taking account of

the recoil particles, we can make an estimate of the the average excitation energy imparted by the protons. It turns out to be close to 230 mev. In this computation it was assumed that the number and average energy of the recoil neutrons are the same as the corresponding values for recoil protons.

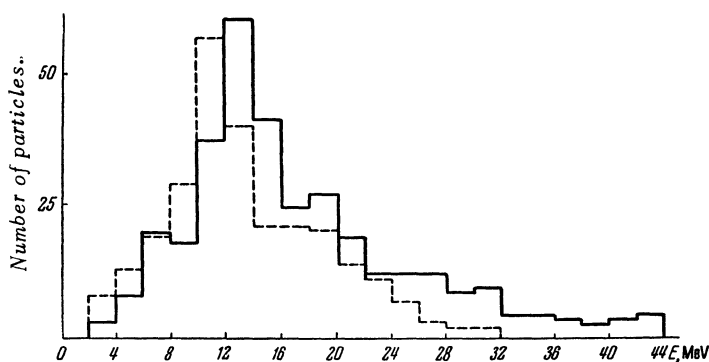


FIG. 5. Energy distribution of α -particles emitted forward (——) and backward (-----).

Computations according to the evaporation theory⁵ predict 5.5 charged particles for an excitation energy of 230 mev. Our measurements give 5.4 particles. Thus our measurements, including the determination of the ratio α/P , the number of charged particles, and the investigation of the shape of the proton spectrum are in agreement with the corresponding data as calculated according to the evaporation theory.

The quantitative data which we have obtained,

such as the fraction of cascade particles and the energy of excitation, are not sufficiently accurate to be used safely in comparing with theoretical calculations. One can only say that the material presented is compatible with general crude ideas about the interaction of fast particles with complex nuclei.

EMISSION OF MESONS

Among the singly charged particles emitted in

disintegrations, there are also π -mesons, whose production intensity increases markedly with the energy of the incident particles.

TABLE VI

	Average energy, mev	Probable energy, mev
Particles emitted forward	16	13
Particles emitted backward	13.7	12

In order to determine the number of charged mesons occurring in a disintegration, all grey tracks in stars formed in an electron-sensitive emulsion of thickness 400-600 μ were measured in order to identify the particles. For this purpose we constructed a calibration curve of grain density versus meson energy from measurements of the number of grains in tracks of π -mesons stopped in the emulsion and in proton tracks. 530 grey tracks in 507 stars were measured by this method, and it was found that 20 of them belonged to π -mesons. Thus, on the average, in one out of 25 disintegrations a single charged π -meson is emitted. Of especial interest is the frequency of emission of two mesons,

TABLE VII

Case number	Track no.	$\bar{\alpha} \cdot 100 \mu$	Grain density dN/dR	Energy				Angle of emergence in $^\circ$	Angle between tracks in $^\circ$
				π -meson		proton			
				from $\bar{\alpha}^\circ$	from dN/dR	from $\bar{\alpha}^\circ$	from dN/dR		
1	1	0.30	52	50 ± 12	30 ± 6	49 ± 12	195 ± 40	21	7
	2	0.237	40	65 ± 16	56 ± 13	59 ± 15	360 ± 100	28	
2	1	0.184	32	88 ± 14	76 ± 10	79 ± 13	500 ± 100	63	14
	2	0.354	62	39 ± 7	20 ± 4	40 ± 7	140 ± 25	49	

formed in a single collision of a proton with a nucleus. The threshold energy for formation of two mesons in the collision of free nucleons is about 600 mev. For collisions of particles with nucleons in the interior of a nucleus the threshold is reduced to ~ 450 mev. In view of this last fact, we undertook a search for cases of production of two mesons, selecting for measurement those disintegrations which contained two or more grey tracks. These tracks had a length greater than 1 mm, and their grain density corresponded to that for tracks of mesons having an energy greater than 10 mev. Among the 3000 disintegrations, two stars were found which each had two π -meson tracks. The characteristics of these tracks are given in Table VII.

Columns 5-8 show the energy values found both from scattering measurements and from grain density measurements, for the two kinds of particles

assumed. There is satisfactory agreement between the energy values determined separately by the two methods only if the particles are π -mesons. Using the value of the cross section for star formation, we can assign an approximate lower limit for the cross section for emission of two charged mesons. This estimate gives a value $\sim 10^{-28}$ cm².

1 E. L. Grigor'ev, Reports of Institute for Nuclear Problems, Academy of Sciences USSR, 1955.
 2 M. Blau, A. R. Oliver, Bull. Am. Phys. Soc. 27, 6 (1952).
 3 N. Page, Proc. Phys. Soc. (London) 63A, 250 (1950).
 4 D. H. Perkins, Phil. Mag. 41, 138 (1950).
 5 K. J. LeCouteur, Proc. Phys. Soc. (London) 65A, 718 (1952).

Other Errata

Page	Column	Line	Reads	Should Read
Volume 4				
38	1	Eq. (3)	$\dots \frac{\pi r^2 \rho^2 \rho_n^2}{\rho_s^2},$	$\dots \frac{\pi r^2 \rho^2 \rho_n}{\rho_s^2},$
196		Date of submittal	May 7, 1956	May 7, 1955
377	1	Caption for Fig. 1	$\delta_{35} = \eta - 21 \cdot \eta^5$	$\delta_{35} = -21 \cdot \eta^5.$
377	2	Caption for Fig. 2	$\alpha_3 = 6.3^\circ \eta$	$\alpha_3 = -6.3^\circ \eta$
516	1	Eq. (29)	$s^2/c^2 \dots$	s/c
516	2	Eqs. (31) and (32)	Replace $A_1 s^2/c^2$ by A_1	
497		Date of submittal	July 26, 1956	July 26, 1955
900	1	Eq. (7)	$\dots \frac{i}{4\pi} \sum_{c, \alpha} \frac{\partial w_a(t, P)}{\partial P^\alpha} \dots$	$\dots 2\pi^2 i \sum_{c, \alpha} \dots$
			(This causes a corresponding change in the numerical coefficients in the expressions that result from the calculation of the effects of the plasma particles on each other).	
804	2	Eq. (1)	$\dots \exp \{-(\bar{T} - V')\}$	$\dots \exp \{-(\bar{T} - V')\tau^{-1}\}$

Volume 5

59	1	Eq. (6)	$v_l (l \partial F_0 / \partial x) + \dots$ where E_l is the projection of the electric field E on the direction l	$\overline{(v \partial F_0 / \partial x)} + \dots$ where the bar indicates averaging over the angle θ and E_l is the projection of the electric field E along the direction l
91	2	Eq. (26)	$\Lambda = 0.84 (1 + 22/A)$	$\Lambda = 0.84 / (1 + 22/A)$
253		First line of summary	$T_1^{204, 206}$	$T_1^{203, 205}$
318	1	Figure caption	$\dots e^2 mc^2 = 2.8 \cdot 10^{-23} \text{ cm},$	$\dots e^2 / mc^2 = 2.8 \cdot 10^{-13} \text{ cm},$
398		Figure caption	\dots to a cubic relation. A series of points etc.	\dots to a cubic relation, and in the region 10–20°K to a quadratic relation. A series of points ●, coinciding with points ○, have been omitted in the region above 10°K.